Eurographics Workshop on 3D Object Retrieval (2014)
B. Bustos, H. Tabia, J.-P. Vandeborre, and R. Veltkamp (Editors)

Symmetry and Fourier Descriptor: A Hybrid Feature For NURBS based B-Rep Models Retrieval

Q-V. Dang, G. Morin and S. Mouysset
University of Toulouse, France

Abstract

As the number of models in 3D databases grows, an efficient 3D models indexing mechanism and a similarity measure to ease model retrieval are necessary. In this paper, we present a query-by-model framework for NURBS based B-Rep models retrieval that combines partial symmetry of the object and the Fourier shape descriptor of canonical 2D projections of the 3D models. In fact, most objects are composed by similar parts up to an isometry. By detecting the dominant partial symmetry of a given NURBS based B-Rep model, we define two canonical planes from which the Fourier descriptors are extracted to measure the similarity among 3D models.

Categories and Subject Descriptors (according to ACM CCS): I.3.5 [Computer Graphics]: Computational Geometry and Object Modelling—Boundary representations I.3.5 [Computer Graphics]: Curve, surface, solid, and object representations—H.3.3 [Information Storage and Retrieval]: Information Search and Retrieval—

1. Introduction

Parametric surfaces, in particular Non-Uniform Rational B-Spline (NURBS), provide a powerful tool for the academic and industrial communities concerned with the design and analysis of objects [DB99]. NURBS based Boundary Representations (NURBS based B-Reps) are industrial standards and are widely used in different domains such as molecular chemistry [BLMP97], 3D geographical information systems [CSM03] and mechanical components design [CH06]. With the explosion of 3D applications in numerous fields of science, the number of 3D models is growing rapidly. Reusing models can help users avoiding to "reinvent the wheel" and increasing the efficiency of industrial product development. Therefore, 3D repositories require algorithms and techniques that are efficient and robust in the back-up organization to index and search the 3D models.

Recently, sketch based approach has become a new trend in 3D shape retrieval where the contours of 3D shapes are extracted and converted into 2D images supplying sketched features to the indexing and searching process [LLJ*10, ERB*12]. This approach provides a friendly interface that allows the users to sketch out a simple 2D shape as a query. The significant success in these works attracted our interests. However, there exists two major limitations that affect the retrieval results. First, they do not define a canonical view that can best describe the overall shapes of similar objects. That is, 2D images are generated from multiple views in [LLJ*10] or are chosen from a set of potential views in [ERB*12]. It does not ensure that the views taken from the similar 3D objects are the same. This can limit the accuracy of the retrieval results in a free sketching context. Second, these algorithms depend on the quality of the representation that it uses to generate contours. Poor models pose a significant problem for contours extraction techniques.

Generally, similarities within a 3D model is a common phenomenon both in natural and in synthetic objects [MPWC12]. Many objects are composed by similar parts up

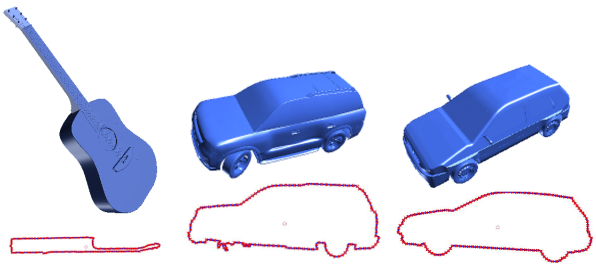

(a) A guitar (b) A 4x4 car (c) A hatchback car

Figure 1: NURBS based B-Rep models and the contours of their projections on global symmetric plane.

DOI: 10.2312/3dor.20141049

to a rotation, a translation or a symmetry. Geometric redundancy is an essential property that 3D designers commonly use in their conceptions. Therefore, the similarity detection within a 3D model can be an important preprocessing step to extract model features that are used to compare the similarity among various models in a database. To clarify this idea, consider now the three NURBS based B-Rep models in Figure 1, we show models in two categories: instrument and car. In each sub-figure, the real model is displayed at the top and the contour of its corresponding projection on global symmetric plane is at the bottom. We can see that the projection on the symmetric plane is a canonical 2D representation that can help us distinguishing shapes between different models. In fact, by applying the D1 distance proposed by Osada et al. [OFCD02], we estimate the shape distribution of each model by evaluating the distances between the samples on its contour to its barycenter. The histograms in Figure 2 shows that the two car models have a similar shape and have a quite different one compared to the guitar.

From this idea, we propose a feature that combines the symmetric property and a 2D shape descriptor of NURBS based B-Rep models. Also, we propose a query-by-model retrieval framework that can be divided into two phases. First, for each of available models, a preprocessing phase estimates its features by detecting its dominant partial symmetry and evaluates the shape descriptors of the silhouettes extracted from the canonical 2D representations. These features are then stored together with the corresponding models. Second, when a model is queried to find other models similar to its shape, it is evaluated the shape descriptor based on its partial symmetry. This shape descriptor is compared to all available shape descriptors to retrieve the desired models. In the context of our work, we suppose that all available 3D models in our databse are closed form and have a dominant partial symmetry.

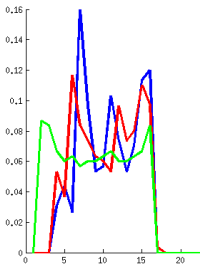

Figure 2: Histograms of shape distributions: (green) the guitar, (blue) the 4x4 car, (red) the hatchback car.

2. Related work

Conceptually, a typical 3D shape retrieval framework consists of a database with an index structure created offline and an online query engine [TV08]. It requires a definition of feature representing the 3D models to ease the similarity comparison between models. In the last decade, several techniques proposed different definitions on 3D shape features; they can be classified in the following approaches: *feature based*, *graph based* and *geometry based* [IJL*05, BKS*05, TV08]. For B-Rep models, the nature of their geometrical structures is a good starting point for direct matching. In an early work, El-Mehalawi et al. [EMM03] proposed an attributed graph approach for retrieving similar designs in a database of mechanical components. In this graph, the nodes represent model surfaces and the links connecting nodes represent the common edge of the corresponding surfaces. Therefore, the model matching problem is reduced to a graph comparison problem. However, graph comparison is NP complete: the comparison becomes costly and inefficient when the number of available models grows or the B-Rep models structures are large and complicated. Chu et al. [CH06] proposed a search scheme which considers form-feature, topological and geometric information. They apply a characteristic that combines the topology graph and the shape distribution to measure the similarity among 3D mechanical components. This scheme seems not to be suitable for our work because the B-Rep objects in a model do not have adjacency information (the structure of these models will be presented in section 3.1). Li et al. [LST*12] propose a combination of the components annontations and the rotational symmetry within B-Rep CAD mechanical models to support partial retrieval. This is a good reference as they use similarity information of a B-Rep model to enhance the search. But our models in this work are more general than their models: they only consider models composed by primitive surfaces.

Symmetry detection for 3D meshes is a well known subject with several approaches as *geometric hashing*, *transformation space voting*, *planar reflective symmetry transform*, *graph based* [MPWC12]. Recently, Cuillière et al. [CFS*11] have presented a method to detect the similarity and the dissimilarity between NURBS based B-Rep models based on the inertia tensor and the control points net of NURBS surfaces. But they do not estimate the transformation between similar surfaces and they consider only the underlying surface but not the edges of B-Rep object. Li [LI11] also proposes an algorithm to detect the symmetry between primitive surfaces within a B-Rep model. In this paper, we propose an algorithm to identify partial symmetries within a NURBS based B-Rep model. This algorithm is independent from the parameterization of underlying NURBS surfaces. Using the dominant partial symmetry and the shape descriptor proposed in [LLJ*10, ERB*12], we derive a hybrid feature to support the shape retrieval.

This paper is organized as follow: section 3 introduces our algorithm for the symmetry detection within a NURBS based B-Rep model, section 4 shows our 3D retrieval framework, we demonstrate our retrieval approach with some experiments in section 5, we finish with the conclusion and some futur works in section 6.

3. Symmetry Detection

In this section, we present our algorithm for detecting the symmetry within a NURBS based B-Rep model. Our algorithm does not only identify automatically repeated faces in the model but also estimates the isometry between them. That is, if two patches P^i, P^j are similar, there exists an isometry T^{ij} so that:

$$P^j = T^{ij}(P^i). \tag{1}$$

We consider isometries as compositions of the canonical isometries, i.e rotations, translations and reflections. They may be direct or indirect. Also, depending on the nature of their linear parts, we characterize the plane symmetries among isometries.

3.1. Structure of NURBS based B-Rep Models

B-Rep (Boundary Representation) is a method for describing the 3D objects by representing each object as a composition of two parts: geometrical and topological entities. Geometrical entities are points, curves and surfaces. These entities are abstracted into topological entities as vertices, edges and faces. Vertices are simply 3D points lying on the surfaces, an edge is a piece of curve bounded by two vertices, and a face is a portion of a surface bounded by multiple edges. In addition, there are two others topological entities: loops and trims. Depending on the loop type (i.e., outer or inner), a loop defines the way to keep or to cut off bounded portions within a surface. A loop is also composed of multiple trims that are directly linked to the edges and which forms a closed boundary.

In our work, a B-Rep object consists of multiple faces and a B-Rep model is composed of multiple B-Rep objects. For instance, the plane model in Figure 3 is composed of B-Reps objects plotted in different colors (figure 3a). Similarly, the plane tail B-Rep object (figure 3b) contains multiple faces. The face in figure 3c is bounded by edges (green) and vertices (red). In addition, the underlying surfaces of B-Rep faces are NURBS surfaces. By definition, a tensor product NURBS surface S of bi-degree (p,q) associated to two knots vectors $\mathbf{u} = \{u_0,\dots,u_n\}$ and $\mathbf{v} = \{v_0,\dots,v_m\}$ and a set of control points $C = \{P_{ij} \mid i \in [0,n-p], j \in [0,m-q]\}$ weighted by $w_{ij} \in \mathbb{R}$, is defined by the following equation:

$$S(u,v) = \frac{\sum_{i=0}^{n-p}\sum_{j=0}^{m-q} N_{i,p}(u)N_{j,q}(v)w_{ij}P_{ij}}{\sum_{i=0}^{n-p}\sum_{j=0}^{m-q} N_{i,p}(u)N_{j,q}(v)w_{ij}}. \tag{2}$$

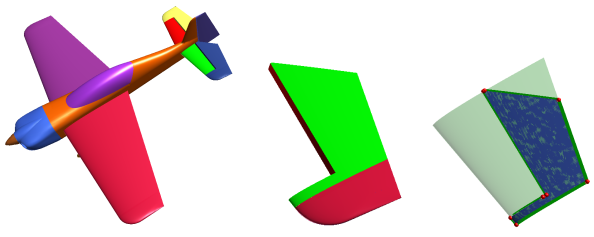

(a) (b) (c)

Figure 3: B-Rep model decomposition. (a) B-Rep objects in a plane model. (b) B-Rep object representing a plane tail. (c) B-Rep entities within a face of the plane tail.

In other words, a B-Rep model contains numerous faces. For detecting symmetry in a model, we first seek symmetric faces within this model. We take advantage of the loop closed form within B-Rep faces, we propose a method for detecting similarity between faces based on the vertices that bound these faces. Moreover, loops in a face must not intersect each others to maintain the validity of the trimmed face. Generally, a face has an outer loop that may contain embedded inner loops. In this work, we only take into account vertices lying on the outer loop of the B-Rep faces.

To ease the notation for the next sections, we denote $M = \{F^i\}, i \in [0,n_F)$, the NURBS based B-Rep model that composed of n_F faces. Each face is defined by $F^i = \{S^i, V^i\}$, where S^i is the NURBS surface used by this face and $V^i = \{v_0^i,\dots,v_n^i\}$ is the set of n vertices that bound F^i. We call the vertices V^i the *corners* of face F^i.

3.2. Algorithm overview

Before entering into the algorithm details, let us introduce some definitions based on the entities of B-Rep objects. Let $F^i = \{S^i, V^i\}$ and $F^j = \{S^j, V^j\}$ two separated faces with the same number of corners (we release this constraint in 3.2.1).

Definition 3.1 F^i and F^j are said *topologically similar* up to a transformation T^{ij} iff T^{ij} maps V^i to V^j:

$$V^j = T^{ij}(V^i). \tag{3}$$

Definition 3.2 F^i and F^j are said *geometrically similar* up to a transformation T^{ij} iff T^{ij} maps S^i to S^j:

$$S^j = T^{ij}(S^i). \tag{4}$$

Note that, if F^i and F^j are topologically similar, we cannot conclude that they are geometrically similar. Similarly, they can be geometrically similar without being topologically similar.

Definition 3.3 F^i and F^j are said *similar* up to a transformation T^{ij} iff they are topological and geometrically similar up to this transformation.

These definitions are the key idea for the overall of our algorithm. Given a B-Rep model $M = \{F^i\}, i \in [0,n_F)$, the algorithm tries to get as more similar faces pairs as possible. It is divided in several steps:

Step 1. Match couples of faces that are topologically similar, i.e. there exists an isometry between the corners of two faces. Let $\Lambda = \{P_k\}$ be the set of pairs of similar faces where $P_k = \{F_k^i, F_k^j\}$ (section 3.2.1).

Step 2. For each P_k, find the least-squares solution R_k and t_k so that

$$V_k^j = R_k * V_k^i + t_k$$

i.e. P_k is topologically similar faces pair (section 3.2.2).
Step 3. For each P_k, estimate the isometry I_k corresponding to R_k and t_k, and keep only the I_k representing a symmetry (section 3.2.3).
Step 4. For each topologically similar faces pair P_k, validate R_k and t_k by applying them to the points on F_k^i and F_k^j. Let $\Delta = \{Q_k\}$ be the set similar faces pairs where $Q_k = \{F_k^i, F_k^j, I_k\}$ (section 3.2.4).
Step 5. Merge equal symmetries in Δ. For each group, relevant isometry and similar patch pairs are extracted. To have the final result for each group, singles faces intersecting the symmetry plane are also tested (section 3.2.5).

3.2.1. Topological faces matching (step 1)

Given two faces $F^i = \{S^i, V^i\}$ and $F^j = \{S^j, V^j\}$, where $V^i = \{v_0^i, \ldots, v_{n-1}^i\}$ and $V^j = \{v_0^j, \ldots, v_{m-1}^j\}$. This step consists of mapping "one-to-one" the corners of V^i into matching corners of V^j where an isometry may exist while reserving the corners orders in corresponding loops. For most cases, similar faces share the same number of corners. However, for some reasons, similar faces may have extra corners in the face loop (e.g to refine corresponding edges). Then, similar faces sometimes have different number of corners while the loops topologies stay unchanged. In the ideal case, $n = m$, it is easy to find out the mappings. We consider all the mappings Tij such that:

$$\sum_{k=0}^{n-1} \left| \|v_k^i - v_{k+1}^i\| - \|v_{m\pm k[n]}^j - v_{m\pm(k+1)[n]}^j\| \right| \qquad (5)$$

where $\|\bullet\|$ is the L_2-norm of Euclidean distance. In contrast, it is more complicated when the number of corners number differs between V^i and V^j. In general, suppose that $n < m$, the isometry testing process finds the optimized subset $V^o = \{v_0^o, \ldots, v_{n-1}^o\} \subset V^j$ cancelling the expression:

$$\sum_{k=0}^{n-1} \left| \|v_k^i - v_{k+1}^i\| - \|v_{n\pm k[n]}^o - v_{n\pm(k+1)[n]}^o\| \right| \qquad (6)$$

In order to derive matching corners between V^i and V^j, we only keep corners of the trim surface where the left and right tangent direction are different enough. This filtering allows to consider only relevant corners. As the mapping between corners is just a necessary condition, a validation on the surfaces will be performed to identify actual mappings (section 3.2.4).

In this step, the process seems to be a greedy approach that has a complexity of $O(N^2)$, where N is the number of faces in the model. For the robustness, only faces with the same bounding boxes volume are tested first for isometry.

3.2.2. Least-Squares Estimation of the Transformation (step 2)

Given two sets V^i and V^o whose corners are mapped according to equation 6, i.e. $v_0^i \mapsto v_0^o, \ldots, v_{n-1}^i \mapsto v_{n-1}^o$, we want to find out the similarity transformation parameters R (rotation) and t (translation) that minimizes the mean squared error of these two point sets:

$$e^2(R,t) = \frac{1}{n} \sum_{k=0}^{n-1} \|v_k^o - (R * v_k^i + t)\|^2. \qquad (7)$$

For simple cases, we solve the linear system $A\overrightarrow{x} = \overrightarrow{b}$ by using the pseudo inverse, where A and $\overrightarrow{b}$ are matrix and vector composed by ordering coordinates of the two set V^i and V^o, $\overrightarrow{x}$ is the solution representing the transformation parameters. But this method fails when the corners of V^i and V^o are coplanar. So we have to find out another method that overcomes this problem. Lorusso et al. [LEF97] compare four algorithms to estimate this transformation. From their comparisons, the singular value decomposition (SVD) of a matrix is the most efficient and robust method. Arun et al. [AHB87] propose an algorithm based on the SVD of a 3×3 matrix, Umeyama [Ume91] refines this algorithm to resolve special cases. The algorithm to estimate the transformations parameters between two points sets V^i and V^o can be resumed as follow:

- Formulate the covariance matrix:

$$H = \sum_{k=0}^{n-1} (v_k^i - \mu_i)(v_k^o - \mu_o)^t. \qquad (8)$$

  where the superscript t denotes the matrix transposition, μ_i and μ_i are the two barycenters of V^i and V^o.
- Find the SVD of H

$$H = USV^t \qquad (9)$$

- Calculate the rotation matrix and the corresponding translation

$$R = VU^t \qquad t = \mu_o - R * \mu_i. \qquad (10)$$

According to [AHB87], if one of the singular values of S is zero (equation 9), i.e. $\lambda_1 > \lambda_2 > \lambda_3 = 0$, we can form another solution R' and t' by introducing the matrix $V' = [v_1, v_2, -v_3]$, where v_1, v_2, v_3 are the three column vectors of V corresponding to the three singular values. We have:

$$R' = V'U^t \quad , \quad t' = \mu_o - R' * \mu_i. \qquad (11)$$

The estimated rotation matrix should be orthogonal in order for the transformation T_{ij} to be an isometry (i.e. to preserve both distances and angles). Additionally, this isometry is direct if $det(R) = 1$ and indirect if $det(R) = -1$.

Note that, this algorithm estimates a unique direct isometry and a unique indirect isometry if the corners number of each set is more than two, i.e. $n > 2$, and the corners in V^i (and V^o) are not colinear. Another interesting advantage of

this algorithm is that it allows the corners to be coplanar. This algorithm meets our needs since the vertices in some faces form a triplet or are coplanar.

In summary, given two sets V^i and V^o whose corners are mapped "one-to-one" (according to equation 6), the least square estimation gives at most two isometries, one direct and another indirect, that transform V^i to V^o. Hence, the faces corresponding to these points set are topologically similar and the corresponding transformation is:

$$T^{ij} = \begin{bmatrix} R^{ij} & t \\ 0 & 1 \end{bmatrix}. \tag{12}$$

3.2.3. Isometry Classification (step 3)

According to [Tis88, Fre10], depending on the nature of the associated fixed points, an isometry T^{ij} can be classified into several classes: translation, rotation, symmetry or combinations of them. We characterize the symmetries by being the isometries with a plane of fixed points.

3.2.4. Isometry Validation (step 4)

Suppose that F^i and F^j are topologically similar up to a reflection T^{ij}. To test if these two faces are also geometrically similar, we have to validate the corresponding transformation on the underlying surfaces. For that, a trivial approach is to validate points sampled from these faces. Effectively, the samples of F^i are transformed by applying T^{ij} to see if the transformed points are the same as the samples of F^j. However, it is challenging to find a mapping "point-to-point" between the samples of two faces according to a given transformation due to two reasons:

- Surface parameterizations are arbitrary and independent from the corners matching.
- Similar faces may have underlying surfaces parameterized differently, i.e, different size of knots vectors, different control points number or different order.

Then, we propose two sampling methods within B-Rep faces used in two scenarios: a *direct sampling* for underlying surfaces with the same parameterization, and a *relative uniform distance* method for underlying surfaces with different parameterizations. The common idea of these two methods is to take samples of the faces based on the corners associated to the inner and outer loops. Furthermore, a face is bounded by edges that are unknown in the underlying surface, some samples may be taken outside the face boundary. Fortunately, as the loop within a B-Rep face is closed, we define a *domain polygon* of 2D parameters (u, v) that bounds the domain of the actual face. A sample is taken if and only if its parameters are inside this polygon.

Direct Sampling

The direct method is involving when the faces have the same parameterization. The parameters of samples within a face are computed based on the corners within the domain polygon. Effectively, we use a barycentric coordinate within a triangle to compute the samples (see Figure 4). For faces having more than three corners, we apply a *constraint Delaunay triangulation* to devise the domain polygon into multiple triangles. With this method, we can easily determine the mapping "point-to-point" between two samples sets by respecting the corners mapping of the two matched faces. Thus, the geometric similarity of the faces is assessed.

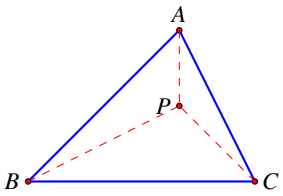

Figure 4: Illustration of barycentric coordinate computation. $P = tA + rB + (1-r-t)C$, with $r+t = 1$ and $r,t \in [0,1]$.

Relative uniform distance sampling

When two similar faces have different parameterizations, it is not feasible to validate the two samples sets gererated by the directed sampling method. In fact, the samples distributions over these two faces are different. We then propose then a stochastic validation based on the shape distribution presented in [OFCD02]. A uniform sampling over u and v parameter spaces cannot generate an equally spaced samples on NURBS surfaces (see Figure 5a). In this method, we use an iterative approach to determine the two parameter gaps based on the distance between two points on the NURBS surface. The distance is defined globally for the actual model. Figure 5b show the equally spaced samples taken over a face.

For the validation, we define a shape function that measures the distance between a point on the surface and the symmetry plane. To construct the shape distribution histogram of a face, we define a B fixed size bins and evaluate the distances of all the taken samples to the symmetry plane. We next count the number of samples that fall into each bin. Let H^i and H^j be the histograms equivalent to the shape distribution of F^i and F^j, we use a correlation metric to measure the similarity between the histograms:

$$d_H(H^i,H^j) = \frac{\sum_{k=1}^{B}(H^i(k)-\overline{H}^i))(H^j(k)-\overline{H}^j))}{\sqrt{\sum_{k=1}^{B}(H^i(k)-\overline{H}^i))^2\sum_{k=1}^{B}(H^j(k)-\overline{H}^j))^2}}, \tag{13}$$

where

$$\overline{H}^k = \frac{1}{B}\sum_{l=1}^{B} H^k(l).$$

If the distance between two histograms is under a threshold, we add the face pair $Q_k = \{F_k^i, F_k^j, I_k\}$ to Δ.

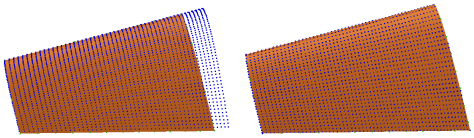

(a) Uniform parameters (b) Relative 3D distances

Figure 5: Two methods of sampling within a trimmed surface.

3.2.5. Isometry Expansion

Now, Δ contains a set of face pairs and corresponding isometries that can share some symmetry planes. These groups of face pairs have to be merged to form the dominant symmetry of the actual model. For that, we define a distance between two isometries as:

$$d(I,I') = \left(1 - \langle \overrightarrow{n}, \overrightarrow{n'} \rangle\right) + \frac{dist(m,P')}{D_{BBox}} + \frac{dist(m',P)}{D_{BBox}}, \tag{14}$$

where $\overrightarrow{n}$ ($\overrightarrow{n'}$), P (P') are normal vector and a point of the symmetry plane corresponding to the isometry I (I'), D_{BBox} is the bounding box diagonal of the actual model, and m (m') is the barycenter of the two faces corners associated to the isometry I (I'). Using this metric (14), we group the face pairs associated with the same symmetry.

The dominant symmetry of the model is the one that has the maximal volume of the bounding box of its symmetric faces. Moreover, there might exist some single faces that are not similar to any other faces but that intersect the dominant symmetry plane. The local symmetry within these faces may contribute to the dominant symmetry. We filter these faces by testing the intersection between the symmetry plane and their bounding box and perform a validation based on the shape distribution of the two set of points that are located in the left and the right of the symmetry plane (using the relative distance sampling).

The figure 6 presents results of the detection of partial symmetries existing in twelve NURBS based B-Rep models. For each sub-figure, the blue and the red patches are the dominant symmetric patches within the models. The smooth parts are the faces contributing to the symmetry, the dot parts are the local symmetries within the faces.

In conclusion, the main idea of our algorithm is to consider the transformation between the faces corners, in order to efficiently filter transformations. If an isometry exists and is a symmetry, it is validated on the faces bounded by the corresponding corners. The validated isometries are merged to identify dominant symmetry of the actual model. An expansion process is performed to get a final result. As a result, for each model, the algorithm gives a symmetry plane and a subset of faces and points of the two symmetric parts. In the next part, this set is used to extract the features of the model to support the model retrieval.

4. Shape Retrieval

In this section, we introduce our proposed feature that encodes the global shape of every model by the Fourier descriptor (FD). This feature can be easily compared to others with a high accuracy. Inspired from the work in [ZL01], we use the results of the symmetry detection and define two canonical planes in which the 2D silhouettes describing the global shapes of 3D models are extracted and in which the FD is evaluated. The following sections describe how we estimate and apply the FD in our work.

4.1. Preprocessing

From the dominant symmetry of a given model, we consider only the symmetric parts (half lies on one side of the symmetry plane, and the other half may be reconstructed by apply-

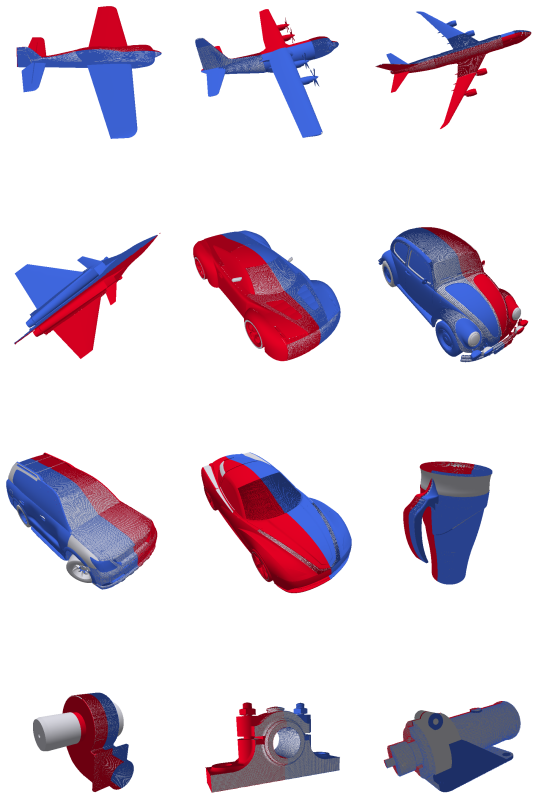

Figure 6: Some results of partial symmetries detection.

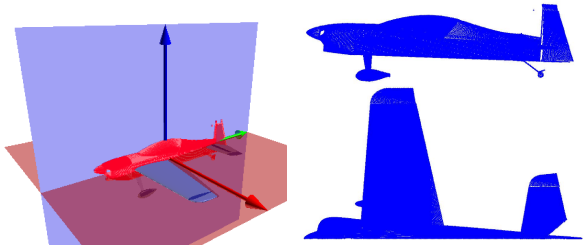

(a) The canonical planes (b) The canonical 2D shapes

Figure 7: Preprocessing step

ing the transformation). The faces are sampled by the uniform distance method. Then, we apply the Principal Component Analysis (PCA) on this points set to get the three principal component vectors. Because of the symmetry, two of the principal components lie in the symmetry plane (and the other one is in the direction of the normal). As showed in the figure 7a, let $\vec{v_1}$ (green), $\vec{v_2}$ (red), $\vec{v_3}$ (blue) be the three principal component vectors in the descending order, the first canonical plane P_c^1 (blue) is defined by the vectors $\vec{v_1}, \vec{v_3}$, the second P_c^2 (red) is defined by the vectors $\vec{v_1}, \vec{v_2}$. The samples set is projected into the two planes orthogonal to the symmetry plane containing two principal vectors to get the canonical 2D shapes of the given model (figure 7b). The silhouettes of these 2D shapes are extracted to estimate the shape descriptors.

4.2. Shape descriptor

From the silhouette of each canonical 2D shape, curve samples are taken following an *equal arc-length sampling*. The figure 8 presents the silhouettes extracted from canonical 2D images in the figure 7b and the corresponding samples. In order to facilitate the use of the fast Fourier transform (FFT), the number of samples N is chosen to be a power-of-two integer. Also, we use the the *centroid distance* as the shape signature to compute the FD, it is defined as:

$$u(t) = \sqrt{[x(t) - x_c]^2 + [y(t) - y_c]^2} \tag{15}$$

where $(x(t), y(t))$ are the coordinates of the ordered samples on the silhouette, $t = 1 \ldots N$; and (x_c, y_c) is the barycenter of the silhouette (that is of the projected 3D sample points). The shape descriptor D_{FD} is a N-tuple of Fourier descriptor F computed over these distances and normalized with respect to DC component F_0:

$$D_{FD} = \left[\frac{|F_1|}{|F_0|}, \frac{|F_2|}{|F_0|}, \ldots, \frac{|F_{N/2}|}{|F_0|} \right]. \tag{16}$$

As mentioned in [ZL01], the centroid distance combining with the normalized FD is translation and scale invariant. These descriptors represent the shape of the object in

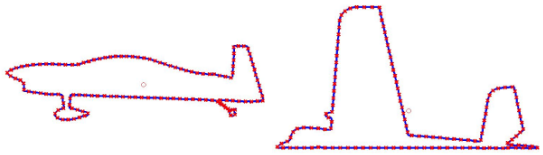

Figure 8: The silhouettes and the samples points.

a frequency domain. The lower frequency descriptors contain information about the general features of the shape, and the higher frequency descriptors contain information about finer details of the shape. Although the number of coefficients generated from the transform is usually large, a subset of the coefficients $(N/2)$ is enough to capture the overall features of the shape.

In our approach, every model has two shape descriptors D_{FD1} and D_{FD2}. The similarity measurement (distance) between two NURBS based B-Rep models M_1 and M_2 is defined as:

$$Sim(M_1, M_2) = \sum_{i=1}^{N/2} |D_{FD1}^1 - D_{FD1}^2| + \sum_{i=1}^{N/2} |D_{FD2}^1 - D_{FD2}^2|. \tag{17}$$

5. Experiments

In this section, we show the results of our proposed retrieval system within a repository of 41 NURBS based B-Rep models that are downloaded from http://www.grabcad.com. Our models fall into four categories: airplane, car, household and animal. Effectively, the shape descriptors of all models are estimated in priori. When a model is queried, its shape descriptors are evaluated and compared to others following the equation 17. Our experimental results are showed in the tables 1 and 2, each row present the query model and its associated results in a descending order of similarity measures. Only the three most relevant models are showed. For airplane, the best matching find all models in the same categories but one. For the cars, the outlier model is a car body (uncompleted car model).

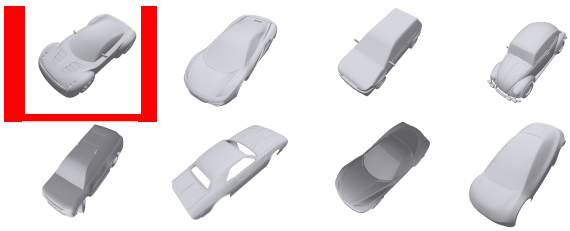

Table 1: Queries for a car and seven best matching.

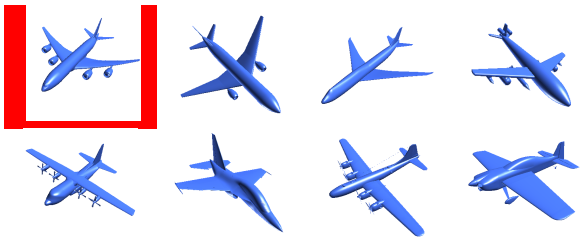

Table 2: Queries for an airplane and seven best matching.

6. Conclusion

In this paper, we propose a hybrid feature combining the symmetry property and the Fourier shape descriptor for 3D model retrieval. There are two main contributions in this work: first, we propose an algorithm to detect the dominant symmetry within a NURBS based B-Rep model; second, we define the two canonical planes that describe the global shapes of a 3D model in 2D representation. The two canonical planes define a common reference where the shape descriptors are computed. This definition of the shape descriptors is independent of the pose of the object. In future work, we plan to consider general isometries. As our similarity detection algorithm can identify all type of transformations within 3D models: rotations, translations, reflections. Each transformation has its own characteristic from which we can elaborate other descriptors to enhance the actual Fourier shape descriptors.

References

[AHB87] ARUN K., HUANG T., BLOSTEIN S.: Least Squares Fitting of two 3D Point Sets. *IEEE transactions on Pattern Analysis and Machine Intelligence PAMI-9*, 5 (1987), 698–700. 4

[BKS*05] BUSTOS B., KEIM D. A., SAUPE D., SCHRECK T., VRANIĆ D. V.: Feature-based Similarity Search in 3D Object Databases. *ACM Comput. Surv. 37*, 4 (2005), 345–387. 2

[BLMP97] BAJAJ C., LEE H. Y., MERKERT R., PASCUCCI V.: NURBS based B-rep models for macromolecules and their properties. In *Proceedings of the fourth ACM symposium on Solid modeling and applications* (1997), ACM, pp. 217–228. 1

[CFS*11] CUILLIÈRE J.-C., FRANÇOIS V., SOUAISSA K., BENAMARA A., BELHADJSALAH H.: Automatic comparison and remeshing applied to {CAD} model modification. *Computer-Aided Design 43*, 12 (2011), 1545–1560. 2

[CH06] CHU C.-H., HSU Y.-C.: Similarity assessment of 3D mechanical components for design reuse. *Robotics and Computer-Integrated Manufacturing 22*, 4 (2006), 332–341. 1, 2

[CSM03] CAUMON G., SWORD JR. C. H., MALLET J.-L.: Constrained Modifications of Non-manifold B-reps. In *Proceedings of the Eighth ACM Symposium on Solid Modeling and Applications* (New York, NY, USA, 2003), SM '03, ACM, pp. 310–315. 1

[DB99] DIMAS E., BRIASSOULIS D.: 3D geometric modelling based on NURBS: a review. *Advances in Engineering Software 30*, 9-11 (1999), 741–751. 1

[EMM03] EL-MEHALAWI M., MILLER R. A.: A database system of mechanical components based on geometric and topological similarity. Part II: indexing, retrieval, matching, and similarity assessment. *Computer-Aided Design 35*, 1 (2003), 95–105. 2

[ERB*12] EITZ M., RICHTER R., BOUBEKEUR T., HILDEBRAND K., ALEXA M.: Sketch-based shape retrieval, 2012. 1, 2

[Fre10] FRESNEL J.: *Méthodes modernes en géométrie*. Hermann, 2010. 5

[IJL*05] IYER N., JAYANTI S., LOU K., KALYANARAMAN Y., RAMANI K.: Three-dimensional shape searching: state-of-the-art review and future trends. *Computer-Aided Design 37*, 5 (Apr. 2005), 509–530. 2

[LEF97] LORUSSO A., EGGERT D., FISHER R.: Estimating 3-D rigid body transformations: a comparison of four major algorithms, 1997. 4

[LI11] LI K.: *Shape Analysis of B-Rep CAD Models to Extract Partial and Global Symmetries*. PhD thesis, 2011. 2

[LLJ*10] LIU Y.-J., LUO X., JONEJA A., MA C.-X., FU X.-L., SONG D.-W.: User-Adaptive Sketch-Based 3-D CAD Model Retrieval. *Automation Science and Engineering, IEEE Transactions on 10*, 3 (2010), 783–795. 1, 2

[LST*12] LI K., SHAHWAN A., TRLIN M., FOUCAULT G., LEON J.: Automated Contextual Annotation of B-Rep Cad Mechanical Components Deriving Technology and Symmetry Information to Support Partial Retrieval. In *Eurographics Workshop on 3D Object Retrieval* (2012). 2

[MPWC12] MITRA N. J., PAULY M., WAND M., CEYLAN D.: Symmetry in 3D Geometry: Extraction and Applications. In *EUROGRAPHICS State-of-the-art Report* (2012). 1, 2

[OFCD02] OSADA R., FUNKHOUSER T., CHAZELLE B., DOBKIN D.: Shape Distributions. *ACM Trans. Graph. 21*, 4 (2002), 807–832. 2, 5

[Tis88] TISSERON C.: *Géométries Affine, Projective et Euclidienne*. Hermann, 1988. 5

[TV08] TANGELDER J. W. H., VELTKAMP R. C.: A survey of content based 3D shape retrieval methods. *Multimedia Tools and Applications 39*, 3 (2008), 441–471. 2

[Ume91] UMEYAMA S.: Least-squares estimation of transformation parameters between two point patterns. *IEEE Transactions on Pattern Analysis and Machine Intelligence 13*, 4 (1991). 4

[ZL01] ZHANG D., LU G.: A comparative study on shape retrieval using Fourier descriptors with different shape signatures. In *Proc. of international conference on intelligent multimedia and distance education (ICIMADE01)* (2001), pp. 1–9. 6, 7